Astrophysical Supercomputing Using Particles
IAU Symposium, Vol. 208, 2003
J. Makino and P. Hut, eds.

Lunar Accretion from an Impact-Generated Disk

Eiichiro Kokubo

National Astronomical Observatory, Osawa, Mitaka, Tokyo, Japan

Shigeru Ida

Tokyo Institute of Technology, Ookayama, Meguro, Tokyo, Japan

Abstract.
We investigate the evolution of a circumterrestrial disk of debris generated by a giant impact on the Earth and the dynamical characteristics of the moon accreted from the disk by using N-body simulation. We find that in most cases the disk evolution results in the formation of a single large moon on a nearly circular orbit close to the equatorial plane of the initial disk just outside the Roche limit. The efficiency of incorporation of disk material into a moon is 10–55%, which increases with the initial specific angular momentum of the disk. These results hardly depend on the initial condition of the disk as long as the disk mass is a few times the present lunar mass and most disk mass exists inside the Roche limit.

1. Introduction

In the "giant impact" scenario, the Moon is accreted from a circumterrestrial disk of debris generated by the impact of a Mars-sized protoplanet with the early Earth (Hartman & Davis 1975, Cameron & Ward 1976). This model has been favored as it can potentially account for major dynamical and geochemical characteristics of the present Earth-Moon system: the system's high angular momentum and depletion of volatiles and iron in the lunar material (e.g., Stevenson 1987). On the other hand, the recent studies of planetary formation revealed that in the late stage of planetary accretion, protoplanets are formed through runaway growth of planetesimals (e.g., Wetherill & Stewart 1989; Kokubo & Ida 1998). In the final stage of the terrestrial planet formation, collisions among protoplanets with sweeping up of residual planetesimals would be likely. Thus, giant impacts may be plausible events.

Giant impacts have been modeled by using a smoothed-particle hydrodynamics (SPH) (e.g., Cameron & Benz 1991; Cameron 1997). It is found that an impact by a Mars-sized protoplanet usually results in formation of a circumterrestrial debris disk. In most cases, significant amount of the disk material exists within the Roche limit.

The accretion process of the moon from the impact-generated disk was first investigated by Canup & Esposito (1996). They used a gas dynamic (particle-in-a-box) model that can describe accretion of solid particles in the Roche zone where accretion is partially inhibited by the tidal force of the Earth. They showed that in general many small moonlets are formed initially rather than a single large moon. However, it is difficult to include global effects such as radial migration of lunar material and interaction of formed moons with the disk and collective effects such as the formation of particle aggregates and spiral arms in the gas model. These effects are potentially very important in the evolution of the disk.

In the present paper, we present high-resolution N-body calculation of the lunar accretion from a circumterrestrial disk (Kokubo et al. 2000). In N-body simulation, global and collective effects are automatically taken into account. We show that the typical outcome of the accretion from the disk is the formation of a single large moon as long as most disk mass is initially within the Roche limit.

2. Method of Calculation

In N-body simulation, the orbits of particles are calculated by numerically integrating the equation of motion. For numerical integration, we use the predictor-corrector type Hermite scheme (Kokubo et al. 1998). For the calculation of mutual gravitational force, which is the most expensive part of N-body simulation, we use the special-purpose computer, GRAPE (Makino et al. 1997).

Collisions between particles play an important role in the evolution of a circumterrestrial disk. It is assumed that two colliding particles rebound with a relative rebound velocity $\vec{v}'$, which is determined by the relative impact velocity $\vec{v}$ and the coefficients of restitution: $\vec{v}'_{\rm n} = -\epsilon_{\rm n}\vec{v}_{\rm n}$ and $\vec{v}'_{\rm t} = \epsilon_{\rm t}\vec{v}_{\rm t}$, where ϵ is the coefficient of restitution $(0 \leq \epsilon \leq 1)$ and the subscripts n and t represent normal and tangential components, respectively. The velocity of each particle after the collision is then calculated based on conservation of momentum. We perform simulations with two values for the normal coefficient of restitution, $\epsilon_{\rm n} = 0.1$ and 0.01; the tangential component is fixed at $\epsilon_{\rm t} = 1$ for simplicity.

The necessary and sufficient conditions for gravitational binding between two orbiting particles are (1) that the Jacobi energy of the two bodies after the collision is negative, and (2) that the centers of mass of both colliding bodies are within their mutual Hill sphere (Kokubo et al. 2000). We consider three different accretion (merging) models. For details of the models, see Kokubo et al. (2000). In principle, the results of all the models are essentially the same. The merged spherical body is assigned a total mass equal to that of the colliding bodies, and its position and velocity are set equal to those of the center of mass of the collision.

We start simulations of lunar accretion assuming a solid particle disk. The initial mass distribution of disk particles was modeled by a power-law mass distribution, $ndm \propto m^{-\alpha}dm$, where n is the number of particles of mass m. The density of disk particles is $\rho = 3.3\mathrm{gcm}^{-3}$ (the bulk lunar density) and the density of the Earth is $\rho_{\oplus} = 5.5\mathrm{gcm}^{-3}$. Disk particles are assumed to be spheres. The initial disk is axisymmetric, with a power-law surface density distribution given by $\Sigma da \propto a^{-\beta}da$, where a is the distance from the Earth, with inner and outer cutoffs, $a_{\rm in}$ and $a_{\rm out}$.

We study the evolution of two initial disk masses, $2M_{\rm L}$ and $4M_{\rm L}$, where $M_{\rm L}$ is the present lunar mass. We also vary the power index of the surface density

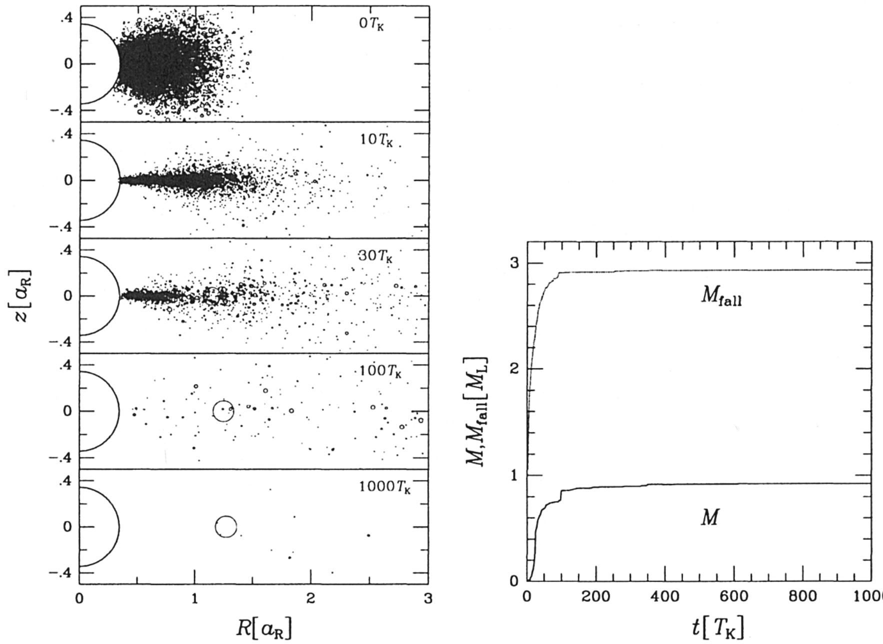

Figure 1. (a: left) Snapshots of the circumterrestrial disk on the $R - z$ plane at $t = 0, 10, 30, 100, 1000T_K$. The semicircle centered at the coordinate origin represents the Earth. Disk particles are shown as circles whose size is proportional to the physical size of disk particles. (b: right) The moon mass M (solid curve) and the mass fallen to the earth M_{fall} (dotted curve) as a function of time.

distribution ($\beta = 1, 3, 5$) and the outer cutoff of the disk ($a_{out} = 0.5, 1, 1.5, 2a_R$), where a_R is the Roche limit radius given by $a_R = 2.456(\rho/\rho_\oplus)^{-1/3}R_\oplus$ and $R_\oplus$ is the Earth radius. The effects of the power index of the mass distribution and the initial velocity dispersion on the result are also tested. The power-law exponent of the mass distribution is chosen to be $\alpha = 0.5, 1.5, 2.5, \infty$, with a dynamic range in mass of $m_{max}/m_{min} = 1000$ for the $\alpha \neq \infty$ cases ($\alpha = \infty$ corresponds to an equal-mass case).

3. Evolution of a Circumterrestrial Disk

We performed 60 simulations with various disk models and 10^4 initial particles. We followed the disk evolution for $1000T_K$, where T_K is the Kepler period at the distance of the Roche limit and $T_K \simeq 7$ hours.

In Figs. 1, we show an example of the simulation. The initial disk has a mass $M_{disk} = 4M_L$ with $\alpha = 1.5$, $\beta = 3$, $a_{in} = R_\oplus$, and $a_{out} = a_R$. We adopted $\epsilon_n = 0.1$. Figure 1a shows snapshots of the circumterrestrial disk in the $R - z$ plane for $t = 0, 10, 30, 100, 1000T_K$. The circumterrestrial disk first flattens through collisional damping and then expands radially. A single large

https://doi.org/10.1017/S0074180900206992 Published online by Cambridge University Press

moon forms around $R \simeq 1.3a_R$ on a nearly non-inclined circular orbit on a time scale of $\sim 100T_K$. These are universal characteristics of the accreted moon and appear to be nearly independent of initial disk conditions.

The mass of the largest moon, M, and the mass fallen to the Earth, M_{fall}, are plotted vs. time in Fig. 1b. The mass of material that escapes from the gravitational field of the Earth is usually smaller than 5% of the initial disk mass. The mass of the moon at $t = 1000T_K$ is $0.9M_L$, while $2.9M_L$ of the initial disk mass has fallen to the Earth. The fraction of the disk mass incorporated into the moon varies with the initial disk conditions.

The disk evolution is divided into two stages, namely, the rapid growth and slow growth stages as seen in Figs. 1. The duration of the rapid growth stage is $\sim 100T_K$, or about a month. In this stage, the redistribution of disk mass through angular momentum transfer supplies material for accretion outside the Roche limit: most of the disk mass falls to the Earth while some of the mass is transported outward. The formation of the moon is almost completed in this stage. The slow growth stage after $\sim 100T_K$ is the "cleaning up stage", where the moon sweeps up and scatters away the residual disk mass.

4. Formation of a Single Moon

In order to see why a single large moon is a typical outcome of the disk evolution, we examine the rapid growth stage in detail. Here we use the rubble pile model in which gravitationally bound particles are not merged but form particle aggregates. The evolution of the spatial structure of the disk is most easily seen by the rubble pile model.

Snapshots of the disk in the $x-y$ plane are shown for $t = 0, 1, 5, 10, 20, 40T_K$ in Figs. 2. The initial condition of the disk here is the same as that shown above except here an equal-mass initial distribution was considered. At $t = 40T_K$, a large bound aggregate with a mass of about one-half the present Moon is formed at $R \simeq 1.3a_R$.

In a disk, self-gravity tends to produce density contrasts, while the random motion of constituent particles and the tidal force (shear) smooth it. When the effect of the tidal force or the random motion overwhelms that of the self-gravity of the disk, the disk is gravitationally stable and density contrasts do not grow in the disk. In fact, a particulate circumterrestrial disk is marginally stable, but instability still plays an important role in the disk evolution.

The evolution of an initially compact disk in the rapid growth stage is described below:

1. The disk contracts through collisional damping of particles.
2. Particle clumps grow inside the Roche limit as the velocity dispersion of particles decreases.
3. The clumps are elongated by Keplerian shear, which forms spiral arms. The spiral arms are smoothed out as they wind up and then the formation of spiral arms is repeated.
4. Particles are transfered to the outside of the Roche limit through the gravitational torque exerted by the spiral arms.

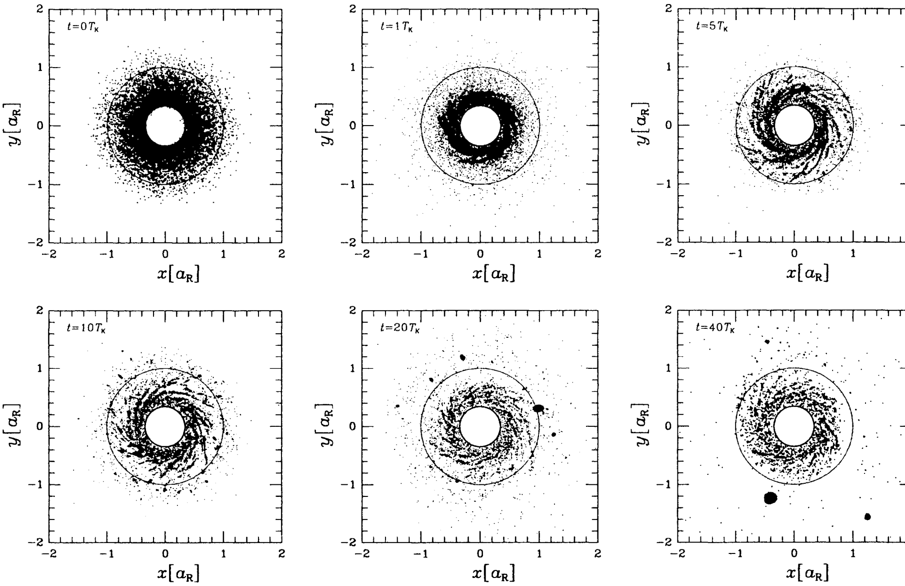

Figure 2. Snapshots of the circumterrestrial disk on the $x-y$ plane at $t = 0, 1, 5, 10, 20, 40T_K$.

5. When a tip of the spiral arm goes beyond the Roche limit, it collapses to form a small moonlet (particle aggregate). The rapid accretion of these small moonlets forms a lunar seed.

6. The seed exclusively grows by sweeping up particles transfered beyond the Roche limit.

7. When the moon becomes large enough to gravitationally dominate the disk, it pushes the rest of the inner disk to the Earth.

As a massive and compact particulate disk evolves in the manner described above, a single large moon forms inevitably.

The time scale of the rapid growth stage is of the order of $100T_K$, relatively independent of the initial conditions. Assuming that the initial disk is contained primarily within the Roche limit, the moon forms from material spreading beyond a_R, so that the time scale of lunar formation is almost equivalent to the time scale of the mass and angular momentum transfer due to the gravitational torque by the spiral arms. In this case, the time scale of lunar accretion is estimated as

$$T_g \sim 10^2 \left(\frac{\Sigma}{0.01 M_\oplus a_R^{-2}}\right)^{-2} \left(\frac{\Delta R}{0.5 a_R}\right)^2 \left(\frac{a}{a_R}\right)^{-9/2} T_K, \tag{1}$$

where ΔR is the radial shift of material due to angular momentum transfer (Kokubo et al. 2000). This time scale agrees well with the results of the N-body simulations. The functional form of T_g shows that the time scale of lunar accretion, depends on not the individual mass of disk particles but rather on the surface density of the disk.

In a compact disk, the lunar seed is formed not by gradual pairwise collision of disk particles but collective particle processes: formation of clumps by gravitational instability, angular momentum transfer due to the gravitational torque due to the spiral arm-like structures, and collapse and collision of particle aggregates. The size of the clumps and the spiral arms are in this case determined by the critical wavelength of the disk, which is a function of the surface density. Mass transfer is driven by the gravitational torque by the spiral arms, whose time scale depends on the surface density. Overall, it is the surface density of the disk, rather than the properties of the individual particles, that governs the evolution of the disk.

5. Dynamical Characteristics of the Moon

We consider the relationship between the dynamical characteristics of the accreted moon and the initial circumterrestrial disk. The orbital elements of the moon are shown in Fig. 3a. The semimajor axis of the moon in all cases is between $a_{\rm R}$ and $1.7a_{\rm R}$, determined mainly by the formation location of the lunar seed and the subsequent interaction with the disk. The lunar seed forms just outside the Roche limit and it is pushed outward from its birth place somewhat by recoil from the inner disk. The eccentricity and inclination of the moon are small due to dynamical friction and collisional damping; in most cases, they are less than 0.1. These values are almost independent of the detailed initial conditions of the disk. The resultant semimajor axis of the moon is small compared with the present lunar semimajor axis. On a longer time scale, the moon migrates outward by the tidal interaction with the Earth, presumably sweeping up outer residual mass.

In Fig. 3b, the mass of the accreted moon, M, scaled by the initial disk mass is plotted vs. the initial specific angular momentum of the disk, $j_{\rm disk}$. The results show that $M/M_{\rm disk}$ increases linearly with $j_{\rm disk}$. This is because in a small $j_{\rm disk}$ disk, a greater amount of mass must fall to the Earth in order for some mass to spread beyond the Roche limit, yielding a smaller final moon. The fraction of material escaping from the Earth also increases with $j_{\rm disk}$, although this fraction is usually less than 5% of the disk mass. The overall yield of incorporation of disk material into a moon ranges from 10–55%.

We explain the relationship between the moon mass M and the specific angular momentum of the circumterrestrial disk, $j_{\rm disk}$, by using a conservation of mass and angular momentum argument. From conservation of mass, we have

$$M_{\rm disk} = M + M_{\rm fall} + M_{\rm esc}, \tag{2}$$

where $M_{\rm esc}$ is the total mass of material that escapes. Conservation of angular momentum gives

$$M_{\rm disk} j_{\rm disk} = Mj + M_{\rm fall} j_{\rm fall} + M_{\rm esc} j_{\rm esc}, \tag{3}$$

where j, $j_{\rm fall}$, and $j_{\rm esc}$ are the mean specific angular momenta of the final moon, the mass that impacts the Earth, and the escaping mass, respectively. This con-

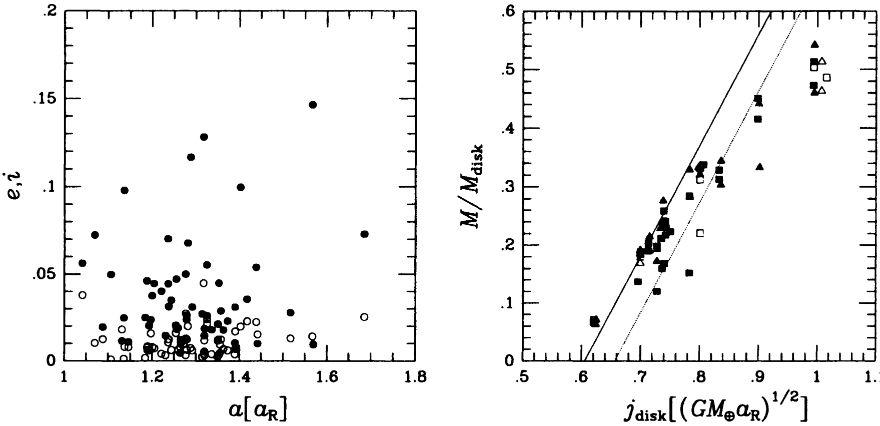

Figure 3. (a: left) The eccentricity (filled circles) and inclination (open circles) of the moon is plotted vs. the semimajor axis of the moon for all the runs. (b: right) The fraction of the initial disk mass incorporated into the moon, $M/M_{\rm disk}$, is plotted against the initial specific angular momentum of the disk, $j_{\rm disk}$. The triangles correspond to runs with an initial disk mass of $M_{\rm disk} = 2M_{\rm L}$ and the squares to runs with $M_{\rm disk} = 4M_{\rm L}$. The filled triangles and squares are for those runs assuming $\epsilon_{\rm n} = 0.1$, and the open ones for those assuming $\epsilon_{\rm n} = 0.01$. The theoretical estimate is also shown for $M_{\rm esc} = 0$ (solid line) and $M_{\rm esc} = 0.05M_{\rm disk}$ (dotted line).

servation argument assumes that the accretion disk is flat and that all material left in Earth orbit has been accreted into a single moon.

From Eqs. (2) and (3), we obtain

$$M = \frac{(j_{\rm disk} - j_{\rm fall})M_{\rm disk} + (j_{\rm fall} - j_{\rm esc})M_{\rm esc}}{j - j_{\rm fall}}. \tag{4}$$

Substituting the mean values of specific angular momenta obtained by the simulations into Eq. (4), yields

$$\frac{M}{M_{\rm disk}} \simeq 1.9\frac{j_{\rm disk}}{\sqrt{GM_\oplus a_{\rm R}}} - 1.1 - 1.9\frac{M_{\rm esc}}{M_{\rm disk}}. \tag{5}$$

This estimate is also shown in Fig. 3b.

Since $M_{\rm esc}$ is always much smaller than $M_{\rm disk}$, we can neglect the $M_{\rm esc}$ terms in Eq. (4). In this case M is a function of j, $j_{\rm fall}$, $j_{\rm disk}$, and $M_{\rm disk}$. However, j and $j_{\rm fall}$ are not free parameters but always have almost the same values since j is determined by the fact that the moon forms just outside the Roche limit and $j_{\rm fall}$ by the fact that remaining particles collide with the Earth. Then, the distribution of the disk mass to the moon and the Earth impactors is determined by the conservation of angular momentum. As the mass of the escapers is small compared with the disk mass, we can predict the mass of the moon from Eq. (5) when the mass and the angular momentum of the disk are given.

The results of the N-body simulation deviate a little from the analytical estimate at low (~ 0.6) and high (~ 1.0) $j_{\rm disk}$. At the low end, the mass of the moon obtained by the simulations is larger than the analytical estimate because the semimajor axis of these moons is smaller than the mean values used in Eq. (4). As the moons in the low $j_{\rm disk}$ cases tend to be smaller in general, they suffer less gravitational recoil from the disk and move outward by a smaller distance, yielding a smaller moon semimajor axis than the mean value. For the high $j_{\rm disk}$ cases, the analytical estimate of the lunar mass is larger than that obtained by the N-body simulations. At the end of these simulations, there are still about 1000 particles exterior to the moon, so that accretion is not yet complete. In fact, the sum of the mass of the moon and the mass of the particles bound to the Earth exterior to the moon (which would likely be the final moon mass) is more consistent with the analytical estimate.

6. Summary

We performed the high-resolution N-body simulations ($N = 10000$) of lunar accretion from various circumterrestrial disks. We found that as a consequence of the evolution of a particulate circumterrestrial disk, a single large moon on a nearly non-inclined circular orbit is formed just outside the Roche limit. This result hardly depends on the initial condition of the disk, as long as $0.62\sqrt{GM_\oplus a_{\rm R}} \le j_{\rm disk} \le 1.0\sqrt{GM_\oplus a_{\rm R}}$, $M_{\rm disk} = 2M_{\rm L}$-$4M_{\rm L}$, and $\epsilon_{\rm n} = 0.01$-0.1, which may include the plausible conditions for the impact-generated disk. The moon is always formed around $a \simeq 1.3a_{\rm R}$. In this case the mass of the moon is predicted simply by conservation of angular momentum from the initial disk. The accretion yields (the fraction of disk material incorporated into the moon) range from 10% to 55%.

The time scale of lunar accretion is of the order of $100T_{\rm K}$ ($\sim$ a month). This time scale hardly depends on the detailed initial conditions of the disk we simulated since the time scales of important processes in lunar formation such as mass transfer is regulated mainly by the surface density of the disk.

References

Cameron, A. G. W. 1997, Icarus, 126, 126

Cameron, A. G. W., & Benz, W. 1991, Icarus, 92, 204

Cameron, A. G. W., & Ward, W. R. 1976, in Lunar and Planetary Science VII (Houston: Lunar and Planetary Institute), 120

Canup, R. M., & Esposito, L. W. 1996, Icarus, 119, 427

Hartmann, W. K., & Davis, D. R. 1975, Icarus, 24, 504

Kokubo, E., & Ida, S. 1998, Icarus, 131, 171

Kokubo, E., Ida, S., & Makino, J. 2000, Icarus, 148, 419

Kokubo, E., Yoshinaga, K., & Makino, J. 1998, MNRAS, 297, 1067

Makino, J., Taiji, M., Ebisuzaki, T., Sugimoto, D. 1997, ApJ, 480, 432

Stevenson, D. J. 1987, AREPS, 15, 271

Wetherill, G. W., & Stewart, G. R. 1989, Icarus, 77, 330